Engineering a superwetting thin film nanofibrous composite membrane with excellent antifouling and self-cleaning properties to separate surfactant-stabilized oil-in-water emulsions

Tian, Miao; Liao, Yuan; Wang, Rong

2019

Tian, M., Liao, Y. & Wang, R. (2019). Engineering a superwetting thin film nanofibrous composite membrane with excellent antifouling and self-cleaning properties to separate surfactant-stabilized oil-in-water emulsions. Journal of Membrane Science, 596, 117721-. https://dx.doi.org/10.1016/j.memsci.2019.117721

https://hdl.handle.net/10356/150367

https://doi.org/10.1016/j.memsci.2019.117721

Engineering a superwetting thin film nanofibrous composite membrane with excellent antifouling and self-cleaning properties to separate surfactant-stabilized oil-in-water emulsions

Miao Tian[1], Yuan Liao[1,3], Rong Wang[1,2*]

1. Singapore Membrane Technology Centre,
Nanyang Environment and Water Research Institute, Nanyang Technological University, 1 Cleantech Loop, Singapore 637141, Singapore

2. School of Civil and Environmental Engineering, Nanyang Technological University, 50 Nanyang Avenue, Singapore 639798, Singapore

3. Sino-Canada Joint R&D Centre for Water and Environmental Safety, College of Environmental Science and Engineering, Nankai University, Tianjin 300071, China

*Corresponding author at: School of Civil and Environmental Engineering, Nanyang Technological University, 639798 Singapore, Singapore. Tel.: +65 6790 5327; fax: +65 6791 0676.
E-mail address: rwang@ntu.edu.sg (R. Wang).

Abstract

In recent years, novel superwetting membranes have gained popularity for oily wastewater treatments via synergy between surface chemistry and topography. However, the water fluxes of the superwetting membranes normally decrease rapidly due to pore clogging and surface fouling, especially when treating surfactant-stabilized oil-in-water emulsions. Herein, a facile strategy is proposed to develop a superwetting thin film nanofibrous composite (TFNC) membrane with remarkable antifouling and self-cleaning properties to effectively separate surfactant-stabilized oil-in-water emulsions. The membrane is composed of an ultrathin carbon nanotubes (CNTs)-polyvinyl alcohol (PVA) composite skin layer, and a highly porous electrospun nanofibrous substrate as well as a non-woven mechanical support. The robust three-dimensional (3D) CNTs composite skin layer were immobilized on the nanofibrous substrate surface by crosslinking the CNTs with PVA. This skin layer serves as a functional barrier to reject oil droplets, which exhibited excellent performance in treating surfactant-stabilized oil-in-water emulsions with a rejection of 95% and a competitive flux of ~60 $Lm^{-2}h^{-1}$ under an ultra-low pressure (20 kPa) in a cross-flow filtration process. Moreover, the CNTs composite layer also protects the membrane surface from fouling. The TFNC membrane possesses outstanding reusability, as the water flux could be recovered by 100% in a continuous cyclic operation without cleaning, which should be attributed to the underwater oil repellence of its superhydrophilic surface and self-cleaning property based on the capillary pumping effect occurred in the micron/nano-channels of the membrane surface.

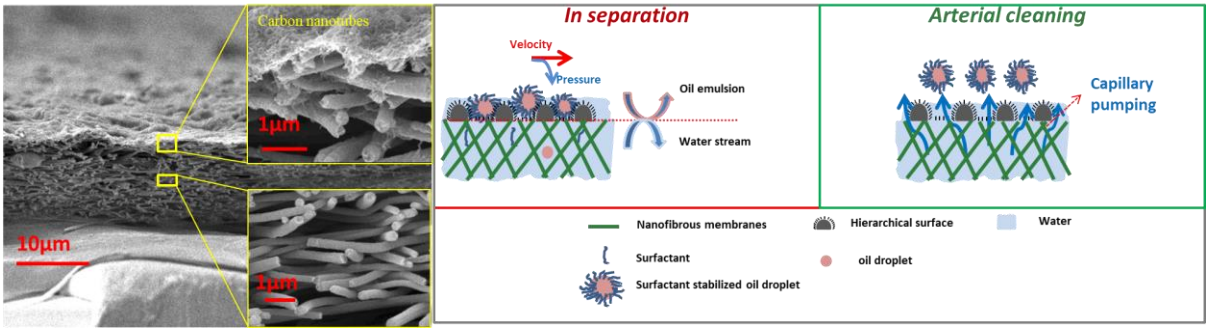

Keywords: surfactant-stabilized oil-in-water emulsion; thin film nanofibrous composite membrane; superwetting; carbon nanotubes; self-cleaning

1 Introduction

Extensive activities in petrochemical, metallurgical, food and pharmaceutical industries have produced increasing amounts of oily wastewater around the world[1, 2]. Due to their adverse impacts on both ecosystem and human health, it is highly desirable yet challenging to treat the oily wastewater using efficient, energy- and cost-effective technologies[1, 3, 4]. The oil/water mixtures may present in multiple forms: oil/water layered solutions (droplet size greater than 150 μm), surfactant-free (droplet size between 20-150 μm) and surfactant-stabilized (droplet size less than 20 μm) oil-in-water and water-in-oil emulsions[5]. The unstable oil/water layered solutions or surfactant-free oil/water emulsions can be readily treated by conventional separation technologies, such as gravity separation, flotation and skimming[6]. The most challenging issue is to separate surfactant-stabilized oil-in-water emulsions which have the oil droplets size down to one micron and are stably dispersed in water by surfactants. A long residence time and even chemical addition are required to enable the conventional separation techniques to be effective. This calls for new promising methods.

To handle surfactant-stabilized oil-in-water emulsions, membrane technology offers an alternative solution because of its acceptable permeate quality, low capital costs, small footprints, absent chemical additions and simple operations[7, 8]. However, in spite of these advantages, the pressurized membrane filtration such as ultrafiltration (UF) and nanofiltration (NF) often encounter serious membrane fouling due to surfactant adsorption and pore clogging by oil droplets, which resulted in a significant reduction in membrane permeability and rejection[9, 10]. To make it worse, the high operating pressure up to several bars required in UF and NF processes not only accelerates the membrane fouling but also increases energy consumption. Additionally, these UF and NF membranes showed poor recoverability after cleaning [10, 11].

Various novel membranes with special wettability have been extensively developed for oil/water separation[12-16]. Inspired by fish scales, the superhydrophilic and underwater superoleophobic surfaces which shows an in-air water contact angle of 0˚ and underwater oil contact angle higher than 150˚ have been fabricated to remove water from oil-in-water mixtures[6, 17-19]. The superhydrophilic materials have water-favourite properties and tend to trap abundant water on their rough surfaces. As water usually exhibits a higher density than oils, the trapped water can serve as a barrier on materials surface to reject oil droplets and greatly reduce the direct contact area between oils and materials, which results in low oil-adhesion and mitigates the fouling propensity. In our previous work, a novel membrane with switchable superwettability for oil and water was developed by electrospinning and surface modification [20, 21]. The membrane can treat various types of oil/water mixtures, including simple layered solutions and emulsions without external driving force or under an ultra-low pressure. However, it displayed a rapid decline of water flux when separating surfactant-stabilized oil-in-water emulsions. Further studies to alleviate membrane fouling and enhance the self-cleaning property of the membrane when treating the surfactant-stabilized oil-in-water emulsions are of great significance.

A number of surface modification approaches, such as self-assembly, chemical etching, atom transfer radical polymerization (ATRP) and chemical vapour deposition (CVD), have been adopted to fabricate the anti-fouling and self-cleaning surfaces[22, 23]. However, these modified membranes required tedious modification steps, special facilities and costly chemicals[13, 24]. Electrospinning is a versatile method to generate continuous nanofibers with a 3D network architecture[19, 25]. The nanofibrous surface with micro-scale roughness could be altered to become hierarchically micro/nano-scaled by further surface modification[26]. Although electrospun membranes have shown promising performance for oil/water separation,

the anti-fouling properties of these membranes require improvement when dealing with surfactant-stabilized oil-in-water emulsions. Formation of a thin film layer on the membrane surface can reduce the opening area between the overlapping point of nanofibers, prevent the intrusion of foulants and enhance surface hydrophilicity, which is expected to enhance antifouling and self-cleaning properties [24, 27].

Recent advances in nanotechnology have expanded the application of nano-materials to membrane technologies. Carbon nanotubes (CNTs) have attracted tremendous interests in membrane development, attributed to its three-dimensional (3D) network structure, outstanding mechanical, thermal, porous and tubular structures [8, 26, 28-31]. Theoretically, functionalized CNTs can increase membrane hydrophilicity and provide better fouling resistance. Recently, the CNTs have been incorporated into a polymer matrix to develop hybrid foams for oil/water separation[32]. However, the incorporation of CNTs in a polymeric matrix requires a large amount of expensive materials (normally 5~10 wt. %), which may hinder their large-scale manufacture[8, 33]. Moreover, most CNTs are easily wrapped or embedded in the thick polymer matrix and their superior intrinsic properties cannot be fully utilized[34].

By taking the advantages of electrospun nanofibrous membranes and CNTs, we report a low-cost and mass-producible approach to fabricate a thin film nanofibrous composite (TFNC) membrane with excellent antifouling and self-cleaning properties, which is specially designed for separating surfactant-stabilized oil-in-water emulsions. The self-cleaning is expected to be achieved via the capillary pumping effect, a nano-scale fluid transport phenomenon in hierarchical nano-channels without the supply of external energy, which has found vast applications spanning from water desalination to biotechnology[35-37]. A tri-layer TFNC membrane was prepared by spraying an ultra-thin CNTs selective layer on the top of

electrospun polyacrylonitrile (PAN) nanofibrous intermediate layer, which was supported by non-woven mechanical support. The CNTs skin layer was cross-linked by poly (vinyl alcohol) (PVA). The as-prepared membrane was characterized comprehensively and batch filtration studies were performed to examine the influence of oil types, applied hydraulic pressure on the water permeability and oil removal efficiency. Moreover, the fouling resistance and self-cleaning property of the membrane were evaluated in a 4-hour continuous crossflow operation.

2 Experimental

2.1 Membrane materials and chemicals

Unless otherwise specified, all chemicals were used as received without further purification. COOH functionalized Multi-walled carbon nanotubes (8-15 nm in diameter, purity of >95 wt%, with a functional group content of 2.5 %) were purchased from Cheaptubes, USA. Poly(ethylene terephthalate) (PET, Grade 3233, Ahlstrom, USA) nonwoven mesh was used as mechanical support. Commercial polyacrylonitrile (PAN, Mw 150,000) purchased from Sigma-Aldrich, Singapore was used to fabricate nanofibrous substrates. N, N-dimethylformamide (DMF, >99.5%) and Isopropyl alcohol (IPA) with analytical grade were provided by Merck, Singapore. Polyvinyl alcohol (PVA, Mw 12,000 to 14,000, 87-88% hydrolyzed) was purchased from Sinopharm Chemical Reagent Co., Ltd. The Polybead ® with a diameter of 100 nm (Cat#16688) was purchased from Polysciences, Inc. to characterize the membrane pore size in crossflow filtration. Petroleum with 18% aromatics basis purchased from Sigma-Aldrich (Singapore) was used to represent industrial oils. Canola oil (100% pure canola oil) was purchased from the supermarket to represent food oils. Tween ® 20 was used as a surfactant to prepare oil-in-water emulsions. Ultrapure water (DI water) with a resistivity of 18.2 MΩ.cm (Millipore Integral 10 Water Purification System) was used to prepare all the

aqueous solutions. A PVDF commercial membrane purchased from GE Osmonics (SKU. PV2HY320F5) was used as a reference.

2.2 Electrospinning of nanofibrous substrate

To prepare a PAN dope solution, PAN polymer powder with the desired amount was dissolved in DMF by stirring at 80 °C. The 8 wt% PAN solution was firstly fed to a spinneret (inner diameter (ID) = 0.75 mm, outer diameter (OD) = 1.59 mm) at a controlled flow rate by a syringe pump and then electrospun to nanofibers on PET non-woven support using an electrospinning apparatus (MJESPIN-08-01, SBTG, Inc, USA) described in our previous work[38, 39]. A thin PAN nanofibrous layer with a thinner nanofiber diameter was then electrospun on the surface of the coarse PAN nanofiber surface by electrospinning the 5 wt% PAN dope which was kept in a fume hood overnight to remove the residual solvent. After that, the nanofibrous support was heat-pressed at 100 °C for 1 h to enhance the integrity of the nanofibrous substrate, which was labelled as PAN. The heat-pressed temperature is selected following the principle that a bit higher than the glass transition temperature (~96 °C) and much lower than the fusion temperature (~322 °C) of the material PAN in order to preserve fiber structure. The detailed electrospun parameters of the nanofibrous substrates are summarized in **Table 1**.

Table 1 Electrospun conditions for preparation of the nanofiber supports.

Sample code	PAN	
	Top	Bottom
Polymer dope	5% PAN	8% PAN
Flow rate (μL/min)	15	15
Applied voltage (kV)	20	20
Working distance (cm)	12	12
Humidity	40±2 %	40±2 %

2.3 Membrane modification

An ultrathin CNTs barrier layer was formed on the aforesaid PAN nanofibrous substrate via spray coating. In brief, we used water as the wetting liquid to occupy the pores in the nanofiber substrates as the membrane is superhydrophilic. A rubber roller was used to remove excessive water on the substrate surfaces. On the top of the wetted PAN nanofibrous support layer, a thin CNTs layer was prepared by spraying a well-mixed CNTs/PVA solution (0.2 wt% CNTs and 0.05 wt% PVA) and 0.05 wt% Glutaraldehyde (GA) solution using a customized spray-coating machine (7000 Dispenser Robot, Spraying Systems Co. (s) PTD LTD)[40]. The pressure in spray coating system was adjusted as well in order not to let the selective layer penetrating into pores. The membrane was then cured at 60 °C for 20 min to cross-link and stabilize the CNTs on the membrane surface. The CNTs amount deposited on the membrane surface was 1 g/m^2 (~2 wt %). The pressure of the coating process should be adjusted in the range of 0.2~1 bar based on a different substrate. The pre-wetting agent may need to prevent penetration of the coating layer into the substrate. The resulted membrane was washed with DI water and stored in water prior to further testing and characterization. The membrane coated with a CNTs barrier layer was coded as CNTs-PAN.

2.4 Characterization of as-prepared composite membranes

Membrane thickness was measured using a micrometer (±4.06 µm accuracy)[41]. The pore size and pore size distribution of the membrane substrate were analysed using a capillary flow porometer (CFP 1500A, Porous Materials, Inc, USA). The membrane's mechanical properties were characterized using a Zwick Universal Testing Machine, USA. The in-air water and underwater oil contact angles of as-fabricated membranes were measured using a goniometer

(Contact Angle System OCA, Data Physics Instruments GmbH, Singapore). The surface and cross-sectional morphologies of the PAN and CNTs-PAN were characterized using a field emission scanning electron microscopy (FESEM, JSM7200F, JEOL Asia Pte Ltd, Japan). The samples were coated with platinum using a sputter coater (JEOL JFC-1600) at 20 mA for 40 s. The surface topography of individual nanofibers was characterized using an XE 100 atomic force microscopy (AFM, Park Systems, Korea). For each sample, an area of 5.0 μm × 5.0 μm was scanned using non-tapping mode. At least three samples of nanofibers were analysed to obtain the average root mean square roughness. Nanofiber diameter was analysed using software *FoxitPDF Reader*. About 100 nanofibers were measured to get the average value and standard deviation.

2.5 Preparation and characterization of oil-in-water emulsions and separation tests

Oil concentration in wastewater generated in the industries mentioned in the introduction section ranges from 50 to 1000 mg/L. Thus, we used 1000 mg/L to simulate the worst situation. The surfactant-stabilized oil-in-water emulsions were prepared using a laboratory blender (Waring Lab Blender). Briefly, 1000 mg of oil and 100 mg of Tween® 20 were added into 1 L DI water, which was blended with a speed of 18000 rpm for 1 min. The weight ratio between oil and surfactant was kept at 10:1. The droplet sizes were measured by a Mastersizer (Malvern Hydro 2000SM). The Total Organic Carbon (TOC) of oil-in-water emulsions and permeates were analysed by Shimadzu TOC Analyzer (Model: TOC-v CSH).

Oil/water separation performance was measured by a cross-flow filtration setup elsewhere. In brief, a membrane coupon with an effective membrane area of 28 cm^2 was compacted using DI water at an applied pressure of 20 kPa for 1 h prior to the water flux measurement. The flow channel dimension of the cell is 1×29×75 mm. Diamond-patterned spacers were placed in both

the feed and permeate fluid channels. The prepared surfactant-stabilized oil-in-water emulsions were pumped by a variable-speed peristaltic pump through the membrane cell at a hydraulic pressure of 20-100 kPa (0.2-1.0 bar) with a velocity of 18 cm/s. Water permeated through the membrane was collected in a beaker and weighted on an electrical balance to calculate membrane flux. The water flux was measured by monitoring the weight change of the permeate. The rejection (R) was calculated according to the TOC difference between the feed and permeate water.

$$R = \left(1 - \frac{C_p}{C_f}\right) \times 100\%$$

where C_f and C_p represent the TOC of the feed and permeate water, respectively.

In the cyclic study of membrane fouling, the cross-flow filtration was stopped to rest the CNTs-PAN membrane for 20 minutes. Then a new cycle test with the same feed solution was started.

3 Results and Discussion

3.1 Membrane structure

The CNTs-PAN membrane with a thickness of 54 μm is composed of a nonwoven support layer, a PAN nanofibrous layer and a crosslinked CNTs layer (**Figure 1a**). The PAN nanofibrous substrate has an open and interconnected porous structure (**Figure 1b)**. The average PAN nanofiber diameter is ~200 nm (**Figure 1c**). An ultrathin crosslinked CNTs layer with a thickness around 200 nm was formed on the top of the substrate through a spray coating system (**Figure 1d**). The FESEM surface morphology of CNTs-PAN (**Figure 1e**) and the image shown in **Figure 1f** confirms that the carbon nanotubes are connected with each other to form a uniform and ultrathin film to fully cover the PAN nanofibrous membrane.

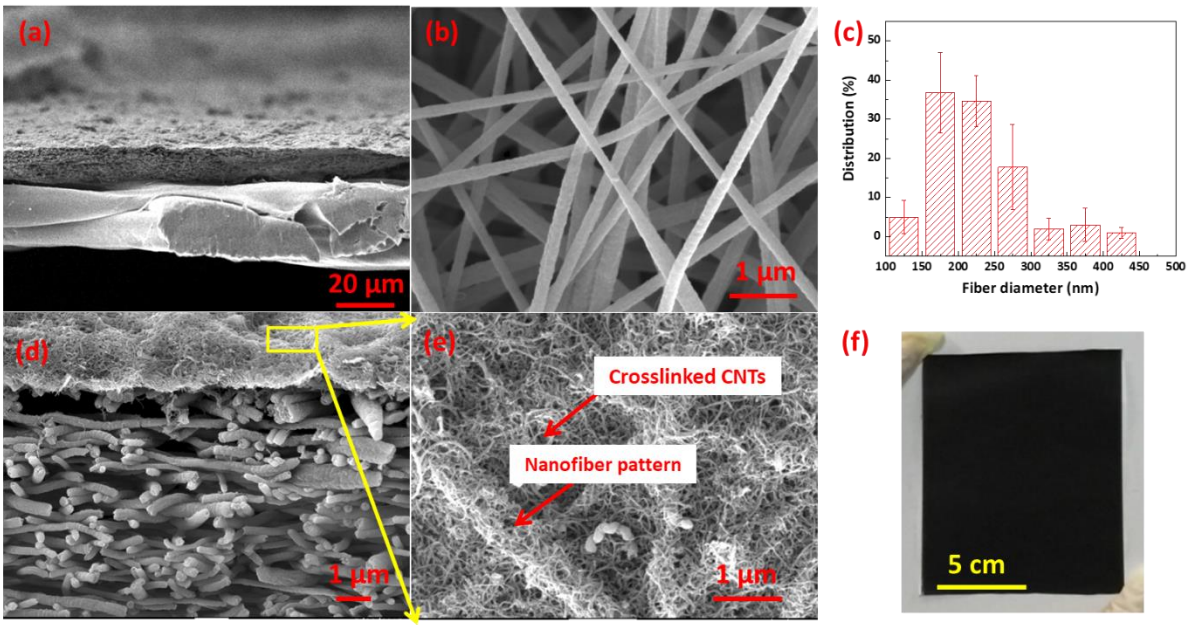

Figure 1 FESEM images of **(a)** cross-sectional CNTs-PAN nanofibrous membrane, **(b)** surface of PAN nanofibrous membrane, **(c)** nanofiber diameter distribution of the PAN nanofibrous membrane, **(d)** cross-sectional FESEM image of the ultrathin crosslinked CNTs coated PAN nanofibrous membrane (CNTs-PAN), **(e)** surface image of the CNTs-PAN membrane. **(f)** photograph of CNTs-PAN membrane (membrane size 12×12 cm).

3.2 CNTs and PVA crosslinking

The COOH group and OH group of CNTs can be linked with -OH group of PVA via Glutaraldehyde with the acid catalyst at 60 ºC[31, 42]. A schematic illustration of the crosslinking mechanism is shown in **Figure 2**. XPS narrow scan spectra of CNTs (**Figure 3 a & b**) and CNTs-PAN membrane (**Figure 3 c & d)** further reveals that C=O /C-O ratio reduced in CNTs-PAN after crosslinking. The reduction of chemical bond C=O is associated with the cross-linking of GA with carboxylic groups present on CNT–COOH, indicating the GA is forming ester bonds with the CNT–COOH. The crosslinking of the CNT–COOH and PVA preventing the CNTs from desorbing and entering the retentate or permeate streams. XPS characterization shows that a decreasing amount of C=O bonds in CNTs-PAN, which confirms the chemical cross-linking between -COOH groups of CNTs and PVA via glutaraldehyde. Moreover, a CNTs selective layer with a coating density of 1g/m^2 was developed in this work by tuning the coating time and dope composition, which is promising for large-scale production.

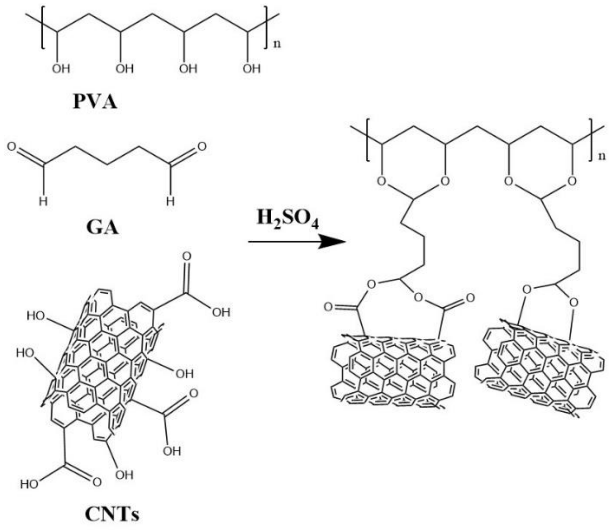

Figure 2 A schematic illustration of the crosslinking mechanism.

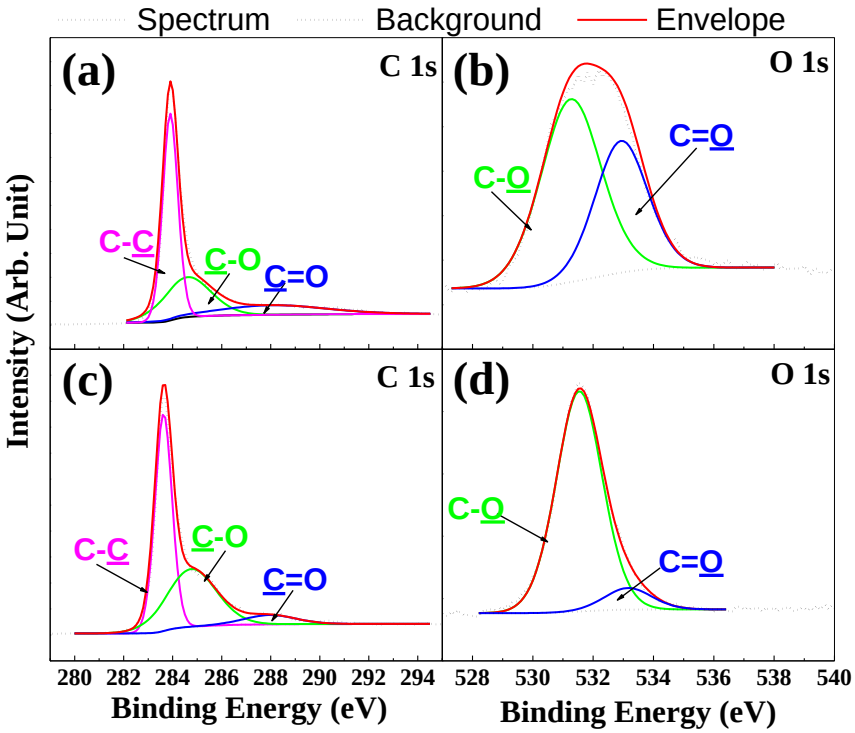

Figure 3 XPS narrow scan spectra of CNTs for elements C 1s (a) and O1s (b); CNTs-PAN membrane for elements C 1s (c) and O 1s (d)

3.3 Membrane intrinsic property

The pore size distributions characterized by the capillary flow porometer of the three membranes are presented in **Figure 4 a**. It can be seen that the CNTs-PAN has a narrow pore size distribution with a mean pore size around 250 nm, which is more uniform and smaller than the PAN support and the commercial membrane. To evaluate the membrane's rejection towards small particles during the cross-flow filtration, commercial uniform polybeads® with particle size of 100 nm was utilized to characterize the membrane pore size. The particle size distribution demonstrates that the average size of the polybeads is 77±0.4 nm (**Figure 4 b**). The CNTs-PAN shows a rejection of 98% to these small rigid polymer beads (**Figure 4 c**). The membrane mechanical strength test also shows that the ultrathin CNTs layer enhances the membrane tensile modulus by 20%, which should be attributed to the super mechanical strength of CNTs and PVA cross-linking (**Figure 4 d).**

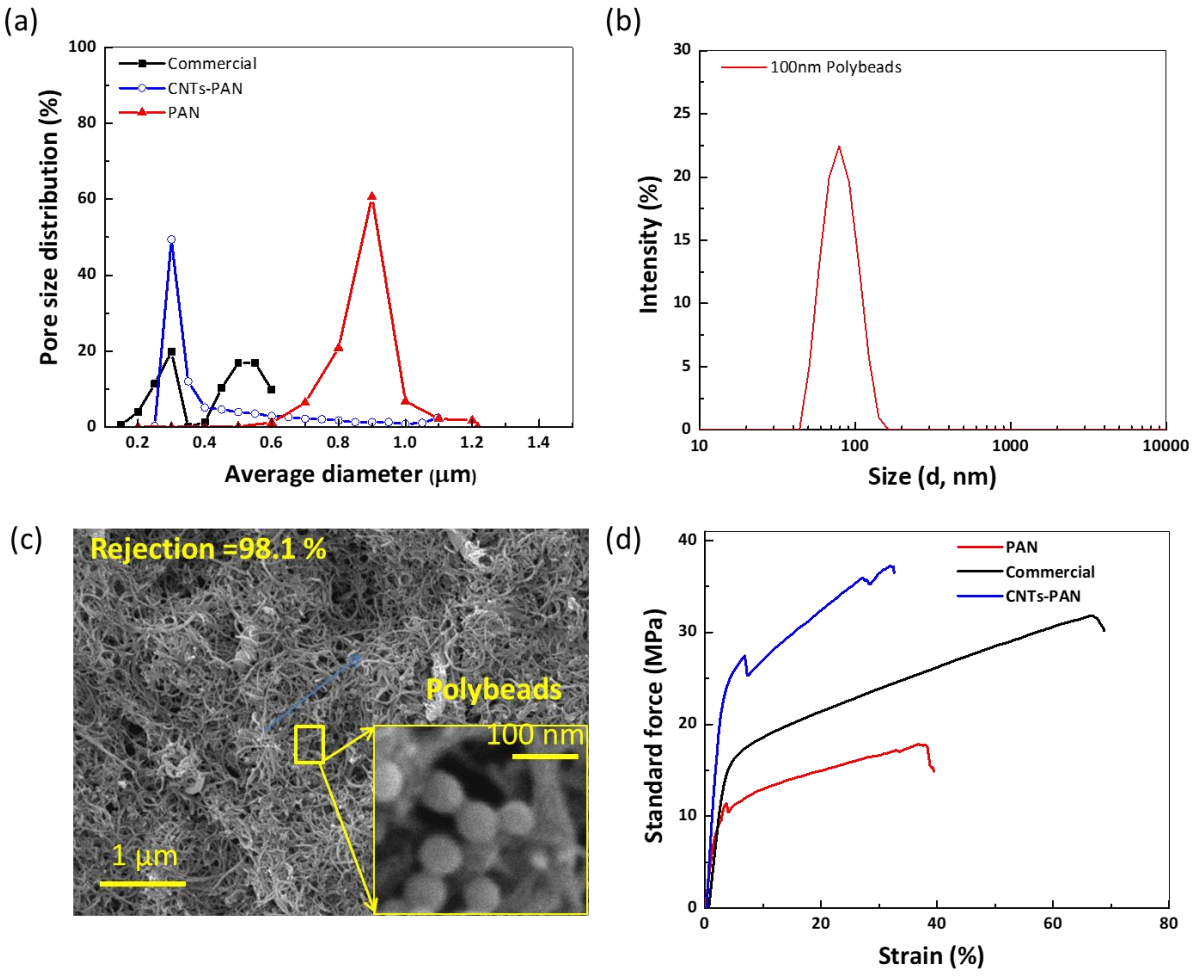

Figure 4 (a) Pore size distribution of the three membranes; (b) 100 nm Polybead® size distribution characterized by zetasizer; (c) FESEM image of the CNTs-PAN membrane after filtration of Polybead®; (d) a group of representing mechanical force vs strain curves of three membranes.

3.4 Surface wetting properties

In-air water contact angles and underwater oil contact angles were used to characterize the surface wettability of as-prepared membranes and the commercial membrane. As shown in **Figure 5 (a)**, after dropping a 5μL water droplet on the membrane surface for 30 seconds, the water contact angles of PAN, CNTs-PAN and the commercial membrane are 24 ± 7°, 32 ± 6° and 94 ± 2°, respectively. After 120 seconds, the water contact angles of PAN and CNTs-PAN membranes are 0° due to their superhydrophilicity and highly porous structure. These surface properties should be attributed to the polar nitrile group in PAN and unreacted hydroxyl/carboxyl groups of PVA crosslinked CNTs[43, 44]. **Figures 5(b)** and **5(c)** show the underwater canola oil and petroleum contact angles of the three membranes. Both PAN and CNTs-PAN membranes showed an underwater superhydrophobicity towards canola oil and petroleum. After cycles of compression, the oil droplet could be eventually broken and a small droplet (marked in the dotted circle) was observed to attach on the micro-structured PAN membrane due to the deformation of the oil droplet under pressure and relatively flat surface microstructure. In contrast, the oil droplet cannot readily attach onto the CNTs-PAN membrane surface even under cycles of physical compression, which should be attributed to its robust hierarchically multi-structured surface shown in **Figure 1(e)**. The surface leads to the lowest contact area of applied oil droplet and thus reduces oil adhesive force significantly. Compared to the PAN and CNTs-PAN membranes, the commercial membrane with flat surface shows lower underwater oil contact angles of 84±10° and 101±15° towards canola oil and petroleum, respectively. A demonstrated video (video 1) is presented in the support information (SI) for a better view of the underwater superoleophobicity.

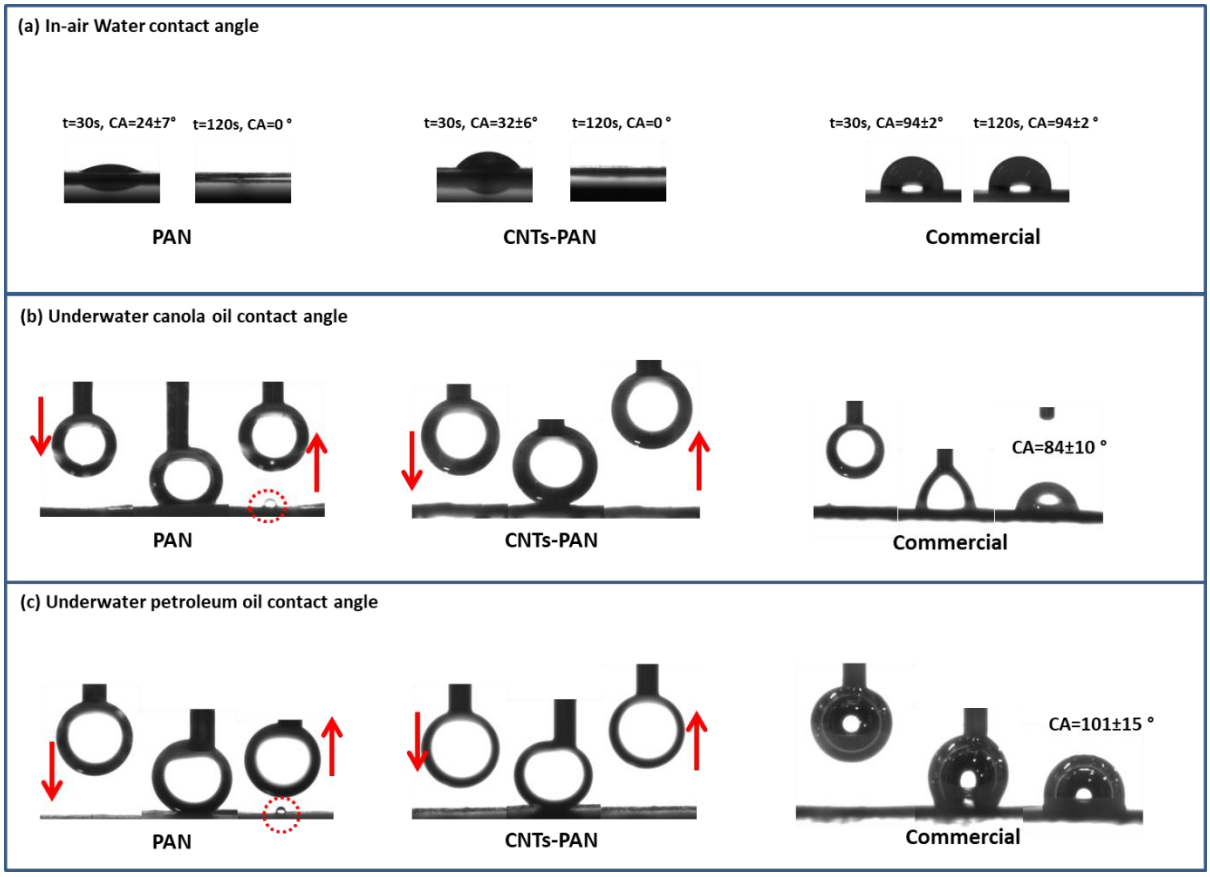

Figure 5 (a) Static water contact angle (WCA), (b) underwater dynamical wetting behaviour of canola oil, (c) underwater dynamical wetting behaviour of petroleum of PAN, CNTs-PAN, and a commercial membrane. The small oil droplets are marked in the dotted circle.

To study the membrane roughness before and after CNTs coating, AFM was used to characterize the membrane surface topography[45]. The combination of CNTs's nanostructure and nanofibrous microstructure can achieve a hierarchical structure as shown in Figure 1(e). This unique structure is essential to enhance the roughness and achieve superwetting properties accompanied by PVA crosslinking. In the underwater condition, this superhydrophilic hierarchical structure is able to absorb water, form a water protective surface layer, provide water pockets between oils and membrane surface, and thus leading to the lowest contact area of applied droplet and resulting in the reduction of adhesive force to oil droplet[26]. It is shown in **Figure 6 (b)** that PAN and CNTs-PAN membranes have a significant higher roughness than the commercial membrane developed by phase inversion technology. The 3D images of the

membrane surfaces show that the additional CNTs layer covers the voids between nanofibers and results in the reduction of overall surface roughness in the scan range of 5 μm*5μm. Interestingly, a pair of representative AFM line profiles in **Figure 6 (c)** shows that although the overall surface roughness value of CNTs-PAN membrane is lower than that of the PAN membrane, it (in green) has a higher peak density (2.6 peaks/μm) than that of PAN membrane (1.8 peaks/μm), indicating its nano-roughness contributing to the hierarchical structure. The peak density of line scan is of great importance for characterizing the roughness of nano composite membrane as the membrane surface roughness is dependent on scan range and location.

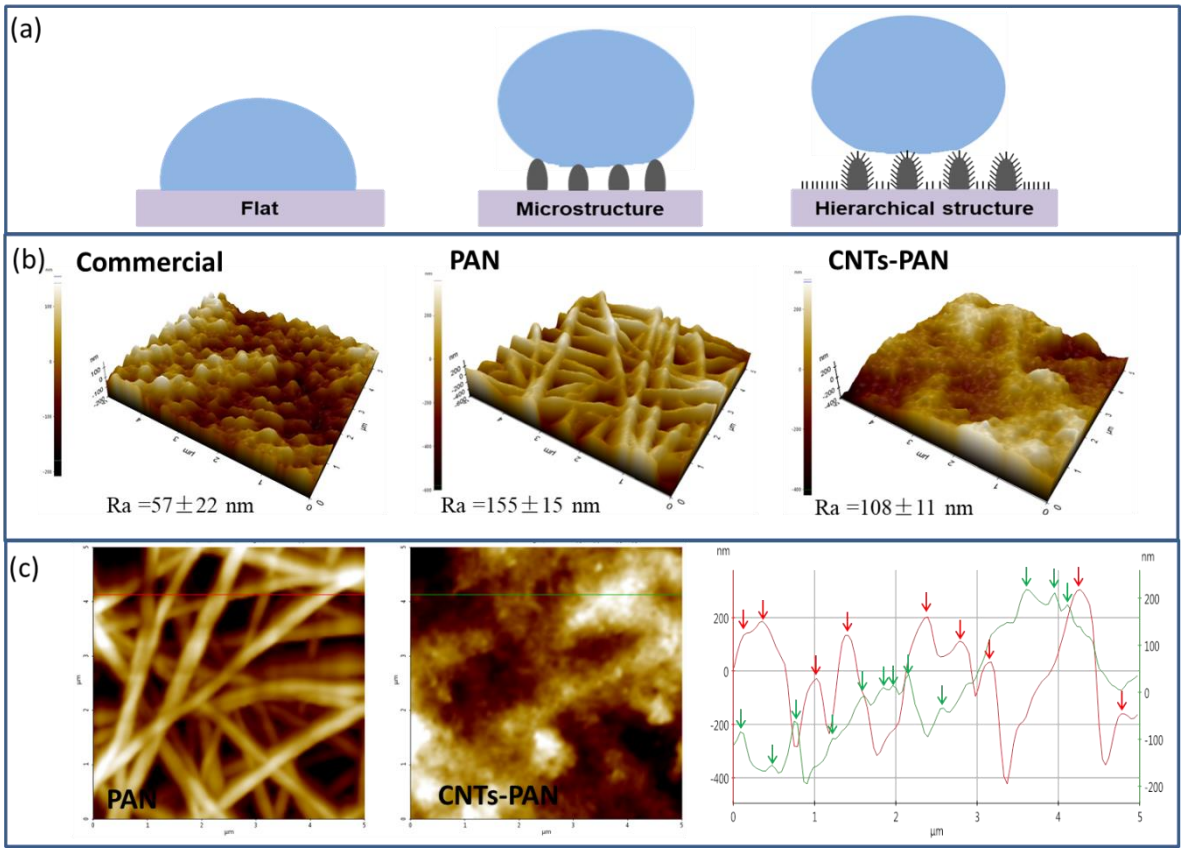

Figure 6 (a) Schematic and wetting of the three different surfaces. The largest contact area between the droplet and the surface is given in flat and microstructured surfaces and is minimized in hierarchical structured surfaces. (b) 3-D surface topography and roughness of the three membrane surfaces by AFM. (c) Surface height maps and corresponding line scan profiles of PAN and CNTs-PAN membrane using an AFM. Height peaks were marked in red (PAN) and green (CNTs-PAN) for calculating the peak density along the scanning length.

3.5 Oil removal from oil-in-water emulsions

As the key performance indexes of a separation membrane, the permeation flux and rejection of CNTs-PAN were assessed, and the results are shown in **Figure 7(a)**. The CNTs-PAN membrane allows continuous water phase to pass through and shows water fluxes of 48 LMH and 60 LMH at an applied pressure of 20 kPa for canola-in-water and petroleum-in-water emulsions, respectively. The water flux of the CNTs-PAN membrane is three times higher than our previously reported membrane when used to treat the same petroleum-in-water emulsions[21]. The CNTs-PAN membrane shows a rejection of 93% and 96% for canola-in-water and petroleum-in-water emulsions, respectively. **Table 2** summarizes the oil droplet size of emulsions. It can be seen that canola oil emulsion has the smallest oil droplet down to 1.46±0.74 μm, and 2.78±0.02 μm for petroleum emulsion. The similar emulsion droplet sizes of the feed solutions before and after tests indicate that emulsions are stable during the tests. Therefore, the difference in permeate flux and rejection of the as-prepared membrane for different oil emulsions depends on the oil droplet size. The membrane shows lower flux in treating canola oil emulsions due to its relatively smaller oil droplets and higher viscosity, thus we used canola oil as the model solution for further study.

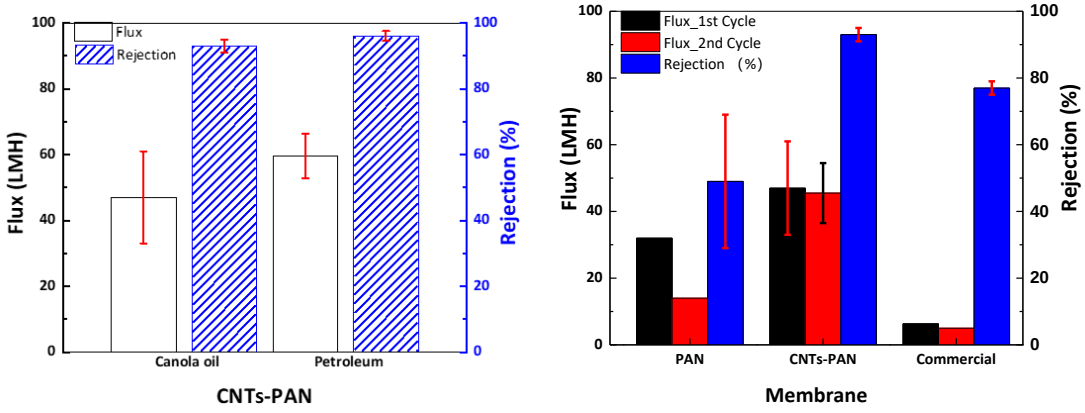

(a) (b)

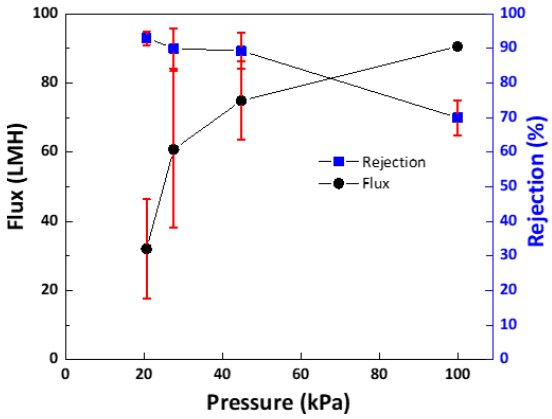

(c)

Figure 7 (a) Permeate fluxes and rejections to various oil-in-water emulsions of membrane CNTs-PAN. (b) Permeate fluxes and rejections of the three membranes, PAN, CNTs-PAN and a commercial membrane with similar pore sizes. Feed emulsion compositions: 1000 ppm oil, 100 ppm surfactant; testing condition: 20 kPa applied pressure, 0.18 m/s surface velocity. (c) Dependence of CNTs-PAN separation performance on working pressure.

Table 2 Oil in water emulsion particle size characterized by Mastersizer

Feed	Feed (1)	Membrane	Feed, 1 hour (2)
	Mean droplet size		Mean droplet size
1000 ppm Petroleum, 100ppm Tween 20	2.78±0.02 µm	CNTs_PAN	3.53±0.12 µm
1000 ppm Canola oil, 100ppm Tween 20	1.46±0.74µm	CNTs_PAN	2.65 ±0.35 µm
1000 ppm Canola oil, 100ppm Tween 20	2.74 ±0. 1µm	Commercial	2.83 ±0.07 µm

Note: (1) Feed samples were collected before the filtration test and was kept for 1 hour before Masterizer characterization. (2) Feed, 1hour: means the samples were collected after a 1-hour crossflow filtration test and characterized by Mastersizer.

Figure 7(b) presents the water flux and rejection to canola oil of the as-prepared PAN, CNTs-PAN membranes and a commercial membrane. The commercial membrane with a mean pore size 0.3 µm shows a flux of 6.3 LMH and 77 ± 2% rejection at 20 kPa. Due to the larger membrane pores and capillary effects, the superhydrophilic nanofibrous membranes usually exhibit better water permeability. The PAN and CNTs-PAN membranes exhibit excellent pure water permeability of 420 ± 51 LMH and 157 ± 64 LMH at a testing pressure of 20 kPa, respectively. In the oil/water separation filtration, the nanofibrous membrane PAN exhibits a comparatively lower flux, lower rejection and lower flux recovery rate due to its large open

surface area, which was eventually fouled by the oil clogging. In contrast, the CNTs-PAN membrane shows a water flux up to 47±14 LMH and 93±2% rejection and a nearly 100% recovery rate in the second cycle without any cleaning. It is believed that the on-top formed additional ultrathin superhydrophilic hierarchical CNTs layer absorbed the water and formed a selective and protective layer to rapidly separate the oil droplets from water, protecting the membrane surface from oil and surfactant clogging, and thus guaranteeing an easy flux recovery. **Figure 7(c)** presents water flux and oil rejection as a function of applied hydraulic pressure of CNTs-PAN membrane. It can be seen that the current membrane can withstand a pressure up to 40 kPa, which indicates its mechanical robustness in the real application. The membrane shows a water flux of 70 LMH and 90% oil rejection at 40 kPa.

3.6 Self-cleaning behaviour

Figure 8(a) shows the normalized permeate fluxes and oil rejections of the PAN membrane, commercial membrane and CNTs-PAN membranes. It should be noted that no physical or chemical cleaning was conducted between the filtration cycles. The flux of the PAN decreases greatly in the first cycle and can only recover 10% of its initial flux in the second cycle. The flux of the commercial membrane decreases over time and loses its initial flux of 20% after the first cycle test and 35% after the second cycle test. The initial flux of the commercial membrane in the second cycle test is only recovered to 86 % after the 20 min rest. Compared with the commercial membrane, the CNTs-PAN membrane possesses nearly full recovery rates of its flux and oil rejection. Moreover, the CNTs-PAN membrane shows even higher separation efficiency of 94%, compared with the commercial membrane (77%). Membrane compaction [21] and oil fouling [7] should be responsible for the flux reduction during both tests**.** After resting the commercial membrane for 20 min, the declined flux due to membrane compaction could be recovered. Thus, the commercial membrane flux increased from 80% to 86% of its

initial flux. However, the flux reduction due to membrane fouling cannot be recovered. In contrast, attributed to the anti-fouling and self-cleaning properties of the superhydrophilic surface and the rebound of membrane compaction, the CNTs-PAN membrane's flux can be fully recovered to its initial flux.

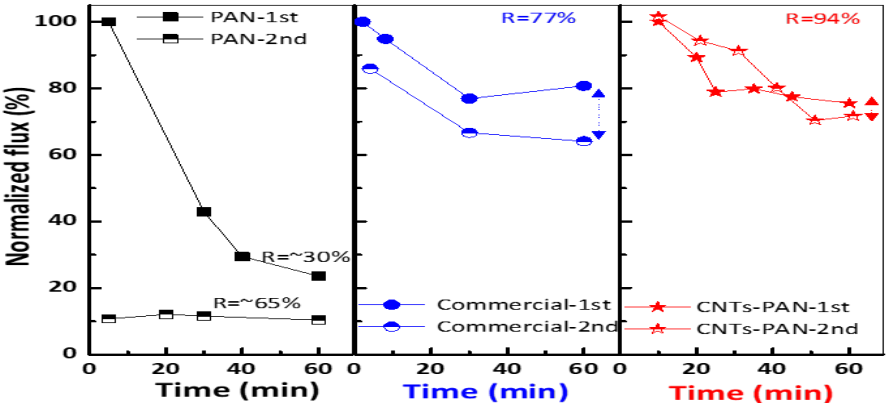

(a)

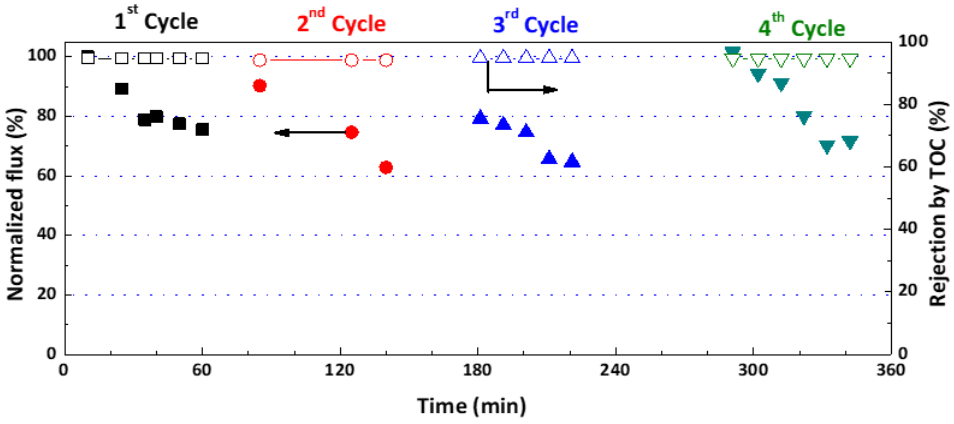

(b)

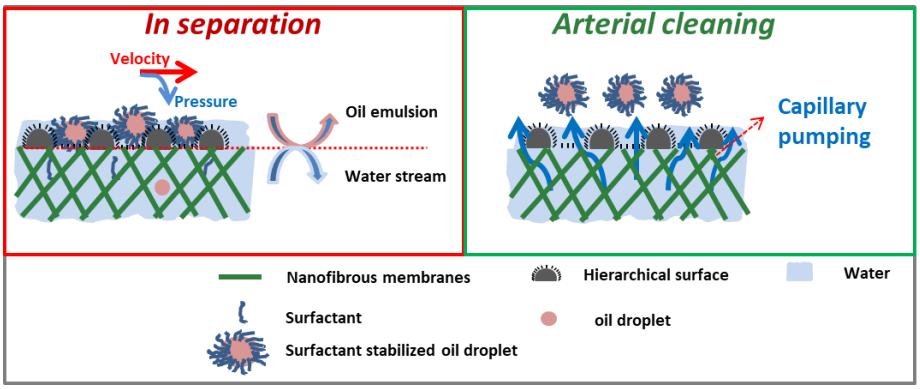

(c)

Figure 8. (a) Normalized permeate flux of a PAN (left), commercial membrane (middle) and CNTs-PAN membrane (right) in a filtration cycle study. Feed emulsion: 1000 ppm canola oil, 100 ppm surfactant. No physical or chemical cleaning process was conducted between 1st and 2nd round test. (b) Long term study of the CNTs-PAN membrane in oil-in-water emulsion separation in a filtration cycle study. Feed emulsion: Feed emulsion: 1000 ppm canola oil, 100 ppm surfactant. No physical or chemical cleaning process was conducted between round tests. (c) Schematic of highly efficient flux recovery and self-cleaning based on capillary pumping assisted with superhydrophilic surfaces and micro channels in CNTs-PAN membranes.

To further confirm this phenomenon, we evaluated the CNTs-PAN membrane in 4-cycle tests as shown in **Figure 8 (b).** The CNTs-PAN membrane shows a promising flux recovery in the four cycles without cleaning. A hypothesis is proposed to explain this excellent flux recovery ability. As illustrated in **Figure 8(c)**, after releasing the pressure applied on membrane surface, the capillary effect in the enormous micro-channels of CNTs layer can draw the permeate water from support layer and force the water up-flow. The up-flow permeate water is able to purge out the surfactant and oil droplets trapped in membrane pores and clean the membrane, which should prolong the membrane lifespan. On the contrary, the surfactant and oil droplets trapped in the membrane with irregular pore structure, high tortuosity and dead-end pore structure, are hard to be cleaned by backwash and consequently contaminate the membrane irreversibly. **Figure 9** presents the schematical drawing to illustrate the possible mechanisms. The video (video 2) presented in the support information (SI) demonstrates that membrane surface remains its underwater superolephobic property well after the long-term filtration test.

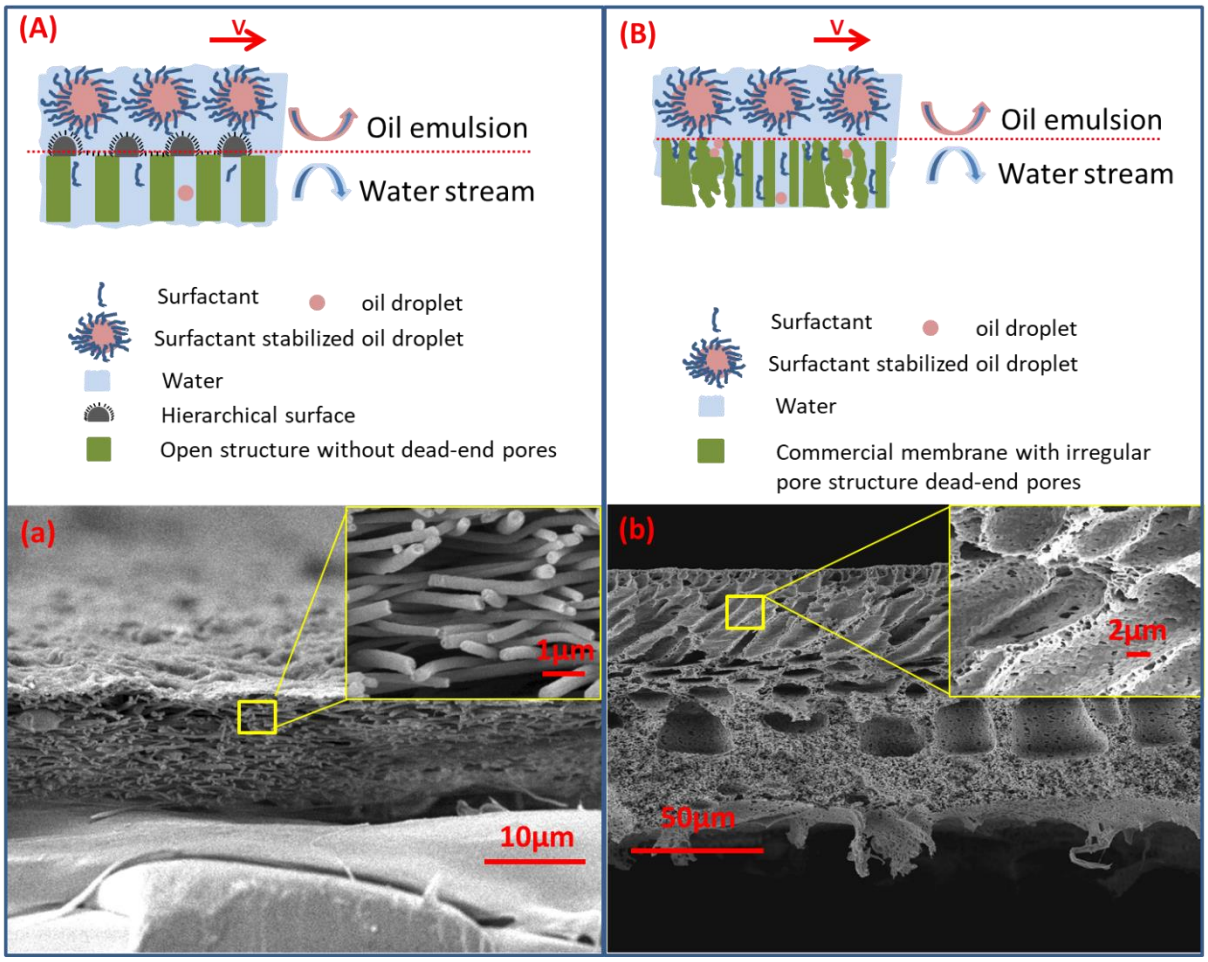

Figure 9 schematically drawing of the surfactant-stabilized oil droplet interaction with (A) CNTs-PAN and (B) commercial membrane with irregular pore structure. The corresponding bottom FESEM group images illustrate the aforesaid (a) open and connected pore structures and (b) irregular pore.

To further demonstrate the self-cleaning properties of CNTs-PAN membrane during oil/water separation process, the surface and cross-sectional FESEM images before and after the 4-hour cross-flow filtration operation are presented in **Figure 10**. The used CNTs-PAN membrane still exhibited a clean micro/nano-structured surface as before, while the commercial membrane was contaminated with the surfactants and oils.

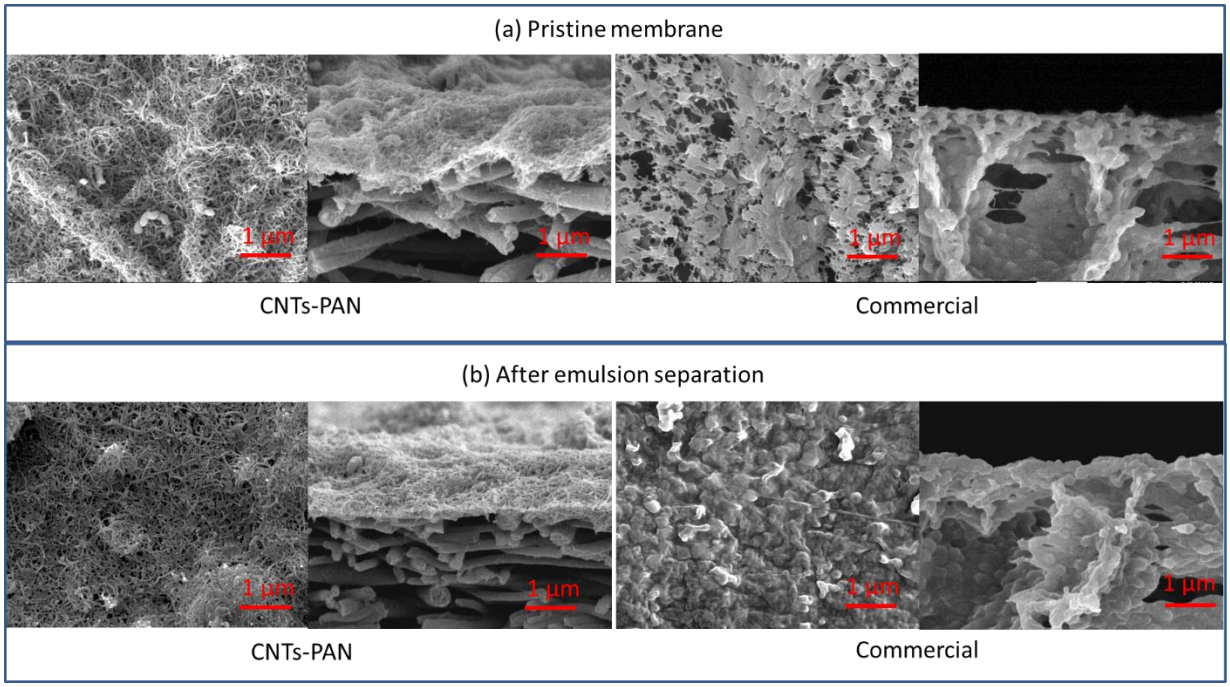

Figure 10 FESEM images of CNTs-PAN hierarchical membrane and the commercial microfiltration membrane (a) before and (b) after the filtration tests.

The as-prepared ultra-thin superhydrophilic CNTs layer can absorb water as a selective layer to remove oil droplets from surfactant-stabilized oil-in-water emulsions, and the function layer can protect the support from contamination by surfactant and oil droplets. Moreover, the highly porous and interconnected CNTs rejection layer and the nanofibrous layer consist of open and active channels for penetrated oil droplet and surfactants, which promise its self-cleaning property by the continuously up-flowed permeate water. In contrast, the dead-end pores of the membranes prepared by conventional phase-inversion method may be blocked by the passed surfactants, which can alter membrane original wettability and reduce membrane selectivity and permeability.

4. Conclusions

A novel TFNC membrane was successfully developed by spraying and crosslinking an ultrathin superhydrophilic CNTs selective layer on the PAN nanofiber matrix. The as-prepared

ultra-thin superhydrophilic CNTs layer can absorb water as a selective layer to remove oil droplets from surfactant-stabilized oil-in-water emulsions, attributed to its in-air superhydrophilic and underwater superoleophobic surface. Meanwhile, the function layer can protect the support from contamination by surfactant and oil droplets. Moreover, the highly porous and interconnected CNTs rejection layer and the nanofibrous layer consist of open and active channels for penetrated oil droplet and surfactants, which promise its self-cleaning property by the continuously up-flowed permeate water. In contrast, the dead-end pores of the membranes prepared by conventional phase-inversion method may be blocked by the passed surfactants, which can alter membrane original wettability and reduce membrane selectivity and permeability. This work provides a new insight for design and development of membranes for oil-in-water emulsion separation and other similar separation processes which suffer from membrane fouling and clogging.

5. Conflicts of interest

There are no conflicts to declare

6. Acknowledgements

We acknowledge funding support from Singapore Economic Development Board to the Singapore Membrane Technology Centre (SMTC).

SUPPORTING INFORMATION

Two demonstrative videos are presented in the support information for a better view of the under superolephobic. Two videos, Video 1 and Video 2, before and after filtration long-term test demonstrate that membrane surface preserve its underwater superolephobic well after the

long-term filtration test. This material is available free of charge via the Internet at http://pubs.acs.org.

References:

Uncategorized References

[1] N.L. Fahrenfeld, H. Delos Reyes, A. Eramo, D.M. Akob, A.C. Mumford, I.M. Cozzarelli, Shifts in microbial community structure and function in surface waters impacted by unconventional oil and gas wastewater revealed by metagenomics, Science of The Total Environment, 580 (2017) 1205-1213.

[2] I.M. Cozzarelli, K.J. Skalak, D.B. Kent, M.A. Engle, A. Benthem, A.C. Mumford, K. Haase, A. Farag, D. Harper, S.C. Nagel, L.R. Iwanowicz, W.H. Orem, D.M. Akob, J.B. Jaeschke, J. Galloway, M. Kohler, D.L. Stoliker, G.D. Jolly, Environmental signatures and effects of an oil and gas wastewater spill in the Williston Basin, North Dakota, Science of The Total Environment, 579 (2017) 1781-1793.

[3] C.H. Peterson, S.D. Rice, J.W. Short, D. Esler, J.L. Bodkin, B.E. Ballachey, D.B. Irons, Long-Term Ecosystem Response to the Exxon Valdez Oil Spill, Science, 302 (2003) 2082-2086.

[4] T. Sirivedhin, L. Dallbauman, Organic matrix in produced water from the Osage-Skiatook Petroleum Environmental Research site, Osage county, Oklahoma, Chemosphere, 57 (2004) 463-469.

[5] Y. Peng, Z. Guo, Recent advances in biomimetic thin membranes applied in emulsified oil/water separation, Journal of Materials Chemistry A, 4 (2016) 15749-15770.

[6] Z. Chu, Y. Feng, S. Seeger, Oil/Water Separation with Selective Superantiwetting/Superwetting Surface Materials, Angewandte Chemie International Edition, 54 (2015) 2328-2338.

[7] B. Chakrabarty, A.K. Ghoshal, M.K. Purkait, Ultrafiltration of stable oil-in-water emulsion by polysulfone membrane, Journal of Membrane Science, 325 (2008) 427-437.

[8] S. Maphutha, K. Moothi, M. Meyyappan, S.E. Iyuke, A carbon nanotube-infused polysulfone membrane with polyvinyl alcohol layer for treating oil-containing waste water, Sci Rep, 3 (2013) 1509.

[9] B. Chakrabarty, A.K. Ghoshal, M.K. Purkait, Cross-flow ultrafiltration of stable oil-in-water emulsion using polysulfone membranes, Chem Eng J, 165 (2010) 447-456.

[10] X. Zhu, A. Dudchenko, X. Gu, D. Jassby, Surfactant-stabilized oil separation from water using ultrafiltration and nanofiltration, Journal of Membrane Science, 529 (2017) 159-169.

[11] L. Yu, M. Han, F. He, A review of treating oily wastewater, Arabian Journal of Chemistry, 10 (2017) S1913-S1922.

[12] Y. Wang, X. Gong, Special oleophobic and hydrophilic surfaces: approaches, mechanisms, and applications, Journal of Materials Chemistry A, 5 (2017) 3759-3773.

[13] S. Wang, K. Liu, X. Yao, L. Jiang, Bioinspired Surfaces with Superwettability: New Insight on Theory, Design, and Applications, Chemical Reviews, 115 (2015) 8230-8293.

[14] Z. Shi, W. Zhang, F. Zhang, X. Liu, D. Wang, J. Jin, L. Jiang, Ultrafast Separation of Emulsified Oil/Water Mixtures by Ultrathin Free-Standing Single-Walled Carbon Nanotube Network Films, Advanced Materials, 25 (2013) 2422-2427.

[15] M.H. Tai, P. Gao, B.Y.L. Tan, D.D. Sun, J.O. Leckie, Highly Efficient and Flexible Electrospun Carbon–Silica Nanofibrous Membrane for Ultrafast Gravity-Driven Oil–Water Separation, ACS Applied Materials & Interfaces, 6 (2014) 9393-9401.

[16] S. Zhang, G. Jiang, S. Gao, H. Jin, Y. Zhu, F. Zhang, J. Jin, Cupric Phosphate Nanosheets-Wrapped Inorganic Membranes with Superhydrophilic and Outstanding Anticrude Oil-Fouling Property for Oil/Water Separation, ACS Nano, 12 (2018) 795-803.

[17] W. Zhang, Y. Zhu, X. Liu, D. Wang, J. Li, L. Jiang, J. Jin, Salt‐induced fabrication of superhydrophilic and underwater superoleophobic PAA‐g‐PVDF membranes for effective separation of oil-in-water emulsions, Angewandte Chemie International Edition, 53 (2014) 856-860.

[18] P.-C. Chen, Z.-K. Xu, Mineral-coated polymer membranes with superhydrophilicity and underwater superoleophobicity for effective oil/water separation, Scientific reports, 3 (2013) 2776.
[19] F. Zhang, W.B. Zhang, Z. Shi, D. Wang, J. Jin, L. Jiang, Nanowire-Haired Inorganic Membranes with Superhydrophilicity and Underwater Ultralow Adhesive Superoleophobicity for High-Efficiency Oil/Water Separation, Advanced Materials, 25 (2013) 4192-4198.
[20] Y. Liao, C.-H. Loh, M. Tian, R. Wang, A.G. Fane, Progress in electrospun polymeric nanofibrous membranes for water treatment: Fabrication, modification and applications, Progress in Polymer Science, 77 (2018) 69-94.
[21] Y. Liao, M. Tian, R. Wang, A high-performance and robust membrane with switchable super-wettability for oil/water separation under ultralow pressure, Journal of Membrane Science, 543 (2017) 123-132.
[22] G.-d. Kang, Y.-m. Cao, Development of antifouling reverse osmosis membranes for water treatment: a review, Water research, 46 (2012) 584-600.
[23] P. Ragesh, V.A. Ganesh, S.V. Nair, A.S. Nair, A review on 'self-cleaning and multifunctional materials', Journal of Materials chemistry A, 2 (2014) 14773-14797.
[24] C.H. Lee, N. Johnson, J. Drelich, Y.K. Yap, The performance of superhydrophobic and superoleophilic carbon nanotube meshes in water–oil filtration, Carbon, 49 (2011) 669-676.
[25] H. Gao, Y. Yang, O. Akampumuza, J. Hou, H. Zhang, X. Qin, A low filtration resistance three-dimensional composite membrane fabricated via free surface electrospinning for effective PM2.5 capture, Environmental Science: Nano, 4 (2017) 864-875.
[26] Y.C. Jung, B. Bhushan, Mechanically durable carbon nanotube− composite hierarchical structures with superhydrophobicity, self-cleaning, and low-drag, ACS nano, 3 (2009) 4155-4163.
[27] W. Qing, X. Shi, Y. Deng, W. Zhang, J. Wang, C.Y. Tang, Robust superhydrophobic-superoleophilic polytetrafluoroethylene nanofibrous membrane for oil/water separation, Journal of Membrane Science, 540 (2017) 354-361.
[28] L. Eskandarian, E. Pajootan, M. Arami, Novel Super Adsorbent Molecules, Carbon Nanotubes Modified by Dendrimer Miniature Structure, for the Removal of Trace Organic Dyes, Industrial & Engineering Chemistry Research, 53 (2014) 14841-14853.
[29] M. Muoth, T. Helbling, L. Durrer, S.W. Lee, C. Roman, C. Hierold, Hysteresis-free operation of suspended carbon nanotube transistors, Nat Nanotechnol, 5 (2010) 589-592.
[30] K. Goh, L. Setiawan, L. Wei, W. Jiang, R. Wang, Y. Chen, Fabrication of novel functionalized multi-walled carbon nanotube immobilized hollow fiber membranes for enhanced performance in forward osmosis process, Journal of membrane science, 446 (2013) 244-254.
[31] A.V. Dudchenko, J. Rolf, K. Russell, W. Duan, D. Jassby, Organic fouling inhibition on electrically conducting carbon nanotube–polyvinyl alcohol composite ultrafiltration membranes, Journal of Membrane Science, 468 (2014) 1-10.
[32] J. Farahbaksh, M. Delnavaz, V. Vatanpour, Investigation of raw and oxidized multiwalled carbon nanotubes in fabrication of reverse osmosis polyamide membranes for improvement in desalination and antifouling properties, Desalination, 410 (2017) 1-9.
[33] X. Wang, X. Chen, K. Yoon, D. Fang, B.S. Hsiao, B. Chu, High flux filtration medium based on nanofibrous substrate with hydrophilic nanocomposite coating, Environmental science & technology, 39 (2005) 7684-7691.
[34] S. Qiu, L. Wu, X. Pan, L. Zhang, H. Chen, C. Gao, Preparation and properties of functionalized carbon nanotube/PSF blend ultrafiltration membranes, Journal of Membrane Science, 342 (2009) 165-172.
[35] M.A. Shannon, P.W. Bohn, M. Elimelech, J.G. Georgiadis, B.J. Marinas, A.M. Mayes, Science and technology for water purification in the coming decades, Nature, 452 (2008) 301-310.
[36] M. Whitby, N. Quirke, Fluid flow in carbon nanotubes and nanopipes, Nature Nanotechnology, 2 (2007) 87-94.
[37] W. Guo, J. Hansson, W. van der Wijngaart, Capillary pumping independent of the liquid surface energy and viscosity, Microsystems & Nanoengineering, 4 (2018) 2.

589 [38] Y. Liao, R. Wang, M. Tian, C. Qiu, A.G. Fane, Fabrication of polyvinylidene fluoride (PVDF)
590 nanofiber membranes by electro-spinning for direct contact membrane distillation, Journal of
591 Membrane Science, 425 (2013) 30-39.
592 [39] M. Tian, C. Qiu, Y. Liao, S.R. Chou, R. Wang, Preparation of polyamide thin film composite
593 forward osmosis membranes using electrospun polyvinylidene fluoride (PVDF) nanofibers as
594 substrates, 118 (2013) 727-736.
595 [40] B. Bolto, T. Tran, M. Hoang, Z. Xie, Crosslinked poly(vinyl alcohol) membranes, Progress in
596 Polymer Science, 34 (2009) 969-981.
597 [41] M. Tian, R. Wang, K. Goh, Y. Liao, A.G. Fane, Synthesis and characterization of high-performance
598 novel thin film nanocomposite PRO membranes with tiered nanofiber support reinforced by
599 functionalized carbon nanotubes, Journal of Membrane Science, 486 (2015) 151-160.
600 [42] R. Rudra, V. Kumar, P.P. Kundu, Acid catalysed cross-linking of poly vinyl alcohol (PVA) by
601 glutaraldehyde: effect of crosslink density on the characteristics of PVA membranes used in single
602 chambered microbial fuel cells, Rsc Adv, 5 (2015) 83436-83447.
603 [43] J. Ge, J. Zhang, F. Wang, Z. Li, J. Yu, B. Ding, Superhydrophilic and underwater superoleophobic
604 nanofibrous membrane with hierarchical structured skin for effective oil-in-water emulsion
605 separation, Journal of Materials Chemistry A, 5 (2017) 497-502.
606 [44] J. Gohil, P. Ray, Polyvinyl alcohol as the barrier layer in thin film composite nanofiltration
607 membranes: Preparation, characterization, and performance evaluation, Journal of colloid and
608 interface science, 338 (2009) 121-127.
609 [45] Y. Huang, H. Li, L. Wang, Y. Qiao, C. Tang, C. Jung, Y. Yoon, S. Li, M. Yu, Ultrafiltration
610 Membranes with Structure-Optimized Graphene-Oxide Coatings for Antifouling Oil/Water
611 Separation, Advanced Materials Interfaces, 2 (2015) 1400433.

612